BJR

https://doi.org/10.1259/bjr.20200884

Received: 19 July 2020 | Revised: 28 October 2020 | Accepted: 04 December 2020

Cite this article as:
Chen L, Hu H, Chen H-H, Chen W, Wu Q, Wu F-Y, et al. Usefulness of two-point Dixon T2-weighted imaging in thyroid-associated ophthalmopathy: comparison with conventional fat saturation imaging in fat suppression quality and staging performance. *Br J Radiol* 2020; **94**: 20200884.

FULL PAPER

Usefulness of two-point Dixon T2-weighted imaging in thyroid-associated ophthalmopathy: comparison with conventional fat saturation imaging in fat suppression quality and staging performance

[1]LU CHEN, MD, [1]HAO HU, MD, [2]HUAN-HUAN CHEN, MD, [1]WEN CHEN, MD, [1]QIAN WU, MD, [1]FEI-YUN WU, MD, PhD and [1]XIAO-QUAN XU, MD, PhD

[1]Department of Radiology, The First Affiliated Hospital of Nanjing Medical University, Nanjing, China
[2]Department of Endocrinology, The First Affiliated Hospital of Nanjing Medical University, Nanjing, China

Address correspondence to:
Dr Fei-Yun Wu
E-mail: *wfy_njmu@163.com*
Xiao-Quan Xu
E-mail: *xiaoquanxu_1987@163.com*

The authors Lu Chen and Hao Hu contributed equally to the work.

Objective: To compare the two-point Dixon T_2 weighted imaging (T_2WI) with conventional fat-sat T_2WI in fat suppression (FS) quality and staging performance for patients with TAO.

Methods: We enrolled 37 thyroid-associated ophthalmopathy (TAO) patients and 15 healthy controls who underwent both coronal two-point Dixon and fat-sat T_2WI. Qualitative (overall imaging quality, FS uniformity) and quantitative [signal intensity ratio of extraocular muscle (EOM-SIR)] parameters were assessed between the two-point Dixon T_2WI and fat-sat T_2WI. Additionally, water fraction of intraorbital fat (IF-WF) was measured on Dixon image. Dixon-EOM-SIR, Fat-sat-EOM-SIR and Dixon-IF-WF values were compared between active and inactive TAO groups, and the diagnostic efficiency for the active phase were evaluated.

Results: Two-point Dixon T_2WI showed significantly higher overall image quality score, FS uniformity score as well as EOM-SIR value than fat-sat T_2WI in both TAO and control groups (all $p < 0.05$). Active TAOs had significantly higher Dixon-EOM-SIR ($p < 0.001$), Fat-sat-EOM-SIR ($p < 0.001$) and Dixon-IF-WF ($p = 0.001$) than inactive TAOs. ROC curves analyses indicated that Dixon-EOM-SIR ≥3.32 alone demonstrated the highest staging sensitivity (75.0%). When integrating Dixon-EOM-SIR ≥3.32 and Dixon-IF-WF ≥0.09, improved staging efficiency and specificity could be achieved (area under the curve, 0.872; specificity, 97.1%).

Conclusion: Compared with conventional fat-sat technique, two-point Dixon T_2WI offers better image quality, as well as improved staging sensitivity and specificity for TAO. Dixon T_2WI is suggested to be used to evaluate the patients with TAO in clinical practice.

Advances in knowledge: Two-point Dixon T_2WI offers better image quality than fat-sat T_2WI. Dixon-EOM-SIR alone demonstrated the highest staging sensitivity. Combining with Dixon-IF-WF showed improved staging efficiency and specificity. Dixon T_2WI is suggested to be used to evaluate TAO patients in clinical practice.

INTRODUCTION

Thyroid-associated ophthalmopathy (TAO) is one of the most common autoimmune inflammatory orbital diseases.[1] The course of the disease includes the active inflammatory phase and the inactive fibrotic phase. The active phase pathologically manifests as mononuclear cell infiltration and edema of the orbital tissues, and is generally responsive to anti-inflammatory treatments.[2] However, the inactive phase, characterized by interstitial fibrosis, collagen deposition and fat infiltration,[3–5] is only rescuable by surgical treatment.[3,6] Therefore, the immediate and accurate discrimination of the two phases is crucial for establishing a proper therapeutic plan and subsequently patients' prognosis.

Recently, fat suppression (FS) T_2 weighted imaging (T_2WI) has been increasingly applied for staging TAO due to high soft tissue resolution, no ionizing radiation, and more distinctively, the ability to detect orbital inflammation and edema.[7,8] Among the array of FS techniques, fat saturation (fat-sat) by mean of chemical shift selective suppression (CHESS) is one of the most common applications. Previous studies based on fat-sat T_2WI have demonstrated that the signal intensity ratios (SIRs) of orbital tissues, especially those of the extraocular muscles (EOMs), were positively correlated with the clinical activity, and could be useful for predicting disease activity.[9–11] However, this conventional FS technique is susceptible to magnetic field inhomogeneity induced by several factors, such as the anatomic geometry and the presence of tissue–tissue and tissue–air interfaces in the orbit and face.[12,13] Thus, the quality of FS with this method is sometimes unsatisfactory, resulting in deviation during quantitative measurement of signal intensity (SI) and consequently limited staging performance.[11,14]

As a novel alternative for FS to circumvent magnetic field inhomogeneity, the Dixon FS technique, based on the water/fat chemical shift difference, by acquiring (at least) two echoes after the exciting radiofrequency pulse, can generate in-phase and opposed-phase images, and water-only and fat-only images after post-processing.[15–17] Thus, essentially it is a water–fat separation method manifesting as improved homogeneity of FS.[18] Moreover, the enablement of fat and water quantification further broadened its applications in various organs and diseases, such as spine, breast, chest and so on.[19–22] However, although the Dixon technique is already routinely used in many examination protocols, the data about its usefulness in the orbit remain scarce.[23,24] Little is known about whether Dixon T_2WI is superior than conventional fat-sat T_2WI when used in orbit, and till now, the performance of Dixon T_2WI in the discrimination of active TAO remains unclear.

Therefore, the aim of our study was to systematically compare the two-point Dixon T_2WI and conventional fat-sat T_2WI in FS quality and staging performance for the patients with TAO.

METHODS AND MATERIALS

Patients

This study was approved by our institutional review board and the informed consent requirement was waived due to its retrospective nature. From July 2018 to November 2019, 37 consecutive patients (mean age, 43.7 ± 4.4 years; male/female ratio,10/27) who were clinically diagnosed with TAO based on Bartley's criteria were enrolled.[25] The inclusion criteria include: (1) pre-treatment orbital MRI, including both coronal two-point Dixon T_2WI and coronal fat-sat T_2WI were available; (2) no history of radiotherapy or surgical decompression; (3) no other orbital pathologies.

The disease activity for each unit of eye was assessed according to the modified 7-point formulation of clinical activity score (CAS) proposed by Mourits et al[26], which includes: spontaneous retrobulbar pain, pain on attempted up or down gaze, redness of the eyelids, redness of the conjunctiva, swelling of the eyelids, inflammation of the caruncle and/or plica and conjunctival edema. Eyes with CAS ≥3 were enrolled in the active phase, otherwise inactive phase. Finally, a total of 40 eyes were defined as active and 34 eyes as inactive. In addition, 15 healthy subjects (mean age, 36.3 ± 11.9 years; male/female ratio, 4/11) were included.

Table 1. Imaging parameters of coronal Dixon and fat-sat T_2WIs

Parameters	Coronal T_2WI	
	Dixon	Fat-sat
Sequence	TSE	TSE
Repetition time (ms)	4000	4000
Echo time (ms)	87	75
Field of view (mm)	180	180
Matrix	179*256	224*320
Number of excitations	2	2
Number of sections	18	18
Section thickness (mm)	3.5	3.5
Acquisition time (min:s)	2:18	2:26

TSE, turbo spin echo; T_2WI, T_2 weighted imaging;fat-sat, fat saturation.

Image acquisition

MRI scans were performed on a 3.0 T MRI system (Magnetom Skyra; Siemens Healthcare, Erlangen, Germany) with a 20-channel head coil. Each patient was instructed to rest in supine position and close eyes to reduce motion-related errors. Two sets of coronal FS imaging sequence (Two-point Dixon T_2WI and fat-sat T_2WI) were performed with comparable imaging parameters. Detailed imaging parameters were summarized in Table 1. Other imaging protocols included axial T_1WI (repetition time [TR]/echo time [TE], 635/6.7 ms), axial and sagittal fat-sat T_2WI (TR/TE, 4000/79–117 ms).

Image analysis

Imaging data of coronal Dixon images of water-only and fat-only and coronal fat-sat T_2WI were analyzed in each unit of eye. Qualitative measurements concerning the quality of FS include: (1) overall image quality for Dixon image of water-only and fat-sat T_2WI, (2) FS uniformity with emphasis on two areas that are prone to incomplete FS (peri-inferior-EOM and temporal-facial regions, respectively) for Dixon image of water-only and fat-sat T_2WI. Both of them were graded by using a 5-point Likert-like scale (1 = poor, 2 = suboptimal, 3 = acceptable, 4 = good, and 5 = excellent).[18]

Quantitative measurements include: (1) SI ratio of extraocular muscle (EOM-SIR) for Dixon image of water-only and fat-sat T_2WI. The EOM-SIR was calculated by using the following formula: EOM-SIR = $SI_{EOM}/SI_{ipsilateral\ temporal\ muscle}$.[27] A circular ROI measuring 5–10 mm^2 was placed in the area of the most inflamed muscle with the highest SI observed by naked eye. The SI of ipsilateral temporal muscle was measured using an

Figure 1. The methods for measurements of EOM-SIR and IF-WF. Coronal Fat-sat T_2WI (a) and two-point Dixon T_2WI of water-only (b) and fat-only (c) in a 32-year-old female with active TAO. For the quantitative measurement of EOM-SIR (a, b), a circular ROI (yellow, 5–10 mm^2) was placed in the area of the most inflamed muscle with the highest signal intensity observed by naked eye and in ipsilateral temporal muscle, respectively. For the quantitative measurement of IF-WF (b, c), a circular ROI (red, 5–10 mm^2) was placed in the area of intraorbital fat. EOM, Extraocular muscle; fat-sat, fat saturation; IF, intraorbital fat; ROI, region of interest; SIR, signal intensity ratio; T_2WI, T_2 weighted; TAO, thyroid-associated ophthalmopathy; WF, Water fraction.

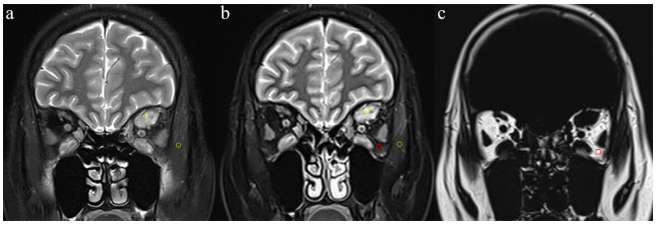

ROI with the similar size. (Figure 1a and b) (2) water fraction of intraorbital fat (IF-WF) for Dixon image. The IF-WF was defined and calculated as: IF-WF = $SI_{water}/(SI_{water} + SI_{fat})$.[28] A circular ROI about 5–10 mm^2 was placed in the area of intraorbital fat. (Figure 1b and c)

Two radiologists (Observer 1: with 6 years of experience in head and neck radiology; Observer 2: with 4 years of experience in head and neck radiology) independently accessed the qualitative parameters and placed the ROIs. They were blinded to study design, acquisition parameters, and clinical information. The measurement results of these two observers were used to assess the inter observer agreement, and the measurement was repeated by observer one with a washout period of at least 1 month, in order to evaluate the intra observer reproducibility.

Statistical analysis

All numeric data were averaged and reported as mean ± standard deviation. Kolmogorov–Smirnov test was used for normality distribution analysis. The differences of qualitative parameters between two-point Dixon and Fat-sat T_2WIs were compared using Wilcoxon signed rank test. Quantitative parameter of EOM-SIR was compared between the two techniques by Wilcoxon signed rank test after correction by averaging values of both eyes.[29] Two-factor split-plot ANOVA was used to evaluate the differences of Dixon-EOM-SIR, fat-sat-EOM-SIR and Dixon-IF-WF between active and inactive phases.[29] ROC curves analyses were performed to evaluate the efficiency of significant quantitative parameters and their combinations in differentiating active from inactive TAOs.

Inter- and intraobserver agreements of qualitative and quantitative parameters were accessed by κ analyses and intraclass correlation coefficient (ICC), respectively. The κ and ICC values range between 0 and 1.00, and values closer to 1.00 represent better reproducibility. They were interpreted as follows:<0.40, poor; 0.41–0.60, moderate; 0.61–0.80, good;≥0.81, excellent. All statistical analyses were carried out with SPSS software package (v. 23.0; IBM, Armonk, NY). A two-sided p-value less than 0.05 was considered statistically significant.

RESULTS

INTER- AND INTRAOBSERVER AGREEMENTS OF QUALITATIVE AND QUANTITATIVE PARAMETERS

Good to excellent inter- and intraobserver reproducibility were obtained when assessing overall image quality and FS uniformity for both two-point Dixon and fat-sat T_2WI (κ ranged from 0.717 to 0.898). Meanwhile, excellent intra- and interobserver agreements were obtained for measurements of EOM-SIRs and Dixon-IF-WF values (ICC ranged from 0. 815 to 0.980). Detailed κ and ICC values were shown in Table 2.

Qualitative and quantitative parameters between Dixon and fat-sat T_2WIs

Two-point Dixon T_2WI showed significantly higher scores of overall image quality and FS uniformity as well as higher value of EOM-SIR than fat-sat T_2WI in both TAO and control groups (all $p < 0.05$). Detailed comparison results between the two techniques were shown in Table 3. Representative Dixon and fat-sat T_2WIs of a patient with active TAO were shown in Figure 2.

Table 2. Inter- and intraobserver reproducibility for qualitative and quantitative parameters

	Intraobserver		Interobserver	
Parameters	Dixon	Fat-sat	Dixon	Fat-sat
Qualitative	κ			
Overall image quality	0.825 (0.593–1.000)	0.816 (0.541–1.000)	0.775 (0.509–0.949)	0.717 (0.404–0.948)
FS uniformity	0.898 (0.636–1.000)	0.846 (0.621–1.000)	0.740 (0.383–1.000)	0.800 (0.580–0.954)
Quantitative	ICC			
EOM-SIR	0.980 (0.969–0.987)	0.976 (0.963–0.984)	0.887 (0.827–0.926)	0.914 (0.869–0.944)
Dixon-IF-WF	0.958 (0.936–0.973)	–	0.815 (0.717–0.879)	–

EOM, extraocular muscle; FS, fat suppression; ICC, intraclass correlation coefficient; IF, intraorbital fat; SIR, signal intensity ratio; WF, water fraction;fat-sat, fat saturation.
Data in parentheses indicate the 95% confidence intervals.

Table 3. Comparisons of qualitative and quantitative parameters between the two techniques in TAO and HC groups

		TAO			HC	
Parameters	Dixon	Fat-sat	*p*	Dixon	Fat-sat	*p*
Qualitive						
Overall image quality	3.81 ± 0.40	3.00 ± 0.41	<0.001[a]	3.80 ± 0.56	3.20 ± 0.41	0.007[a]
FS uniformity	3.89 ± 0.31	2.78 ± 0.42	<0.001[a]	3.93 ± 0.26	2.73 ± 0.59	0.001[a]
Quantitative						
EOM-SIR	3.50 ± 1.42	2.95 ± 1.07	<0.001[a]	2.06 ± 0.32	1.78 ± 0.26	0.001[a]

EOM, extraocular muscle; FS, fat suppression; Fat-sat, fat saturation; HC, healthy control; SIR, signal intensity ratio; TAO, thyroid-associated ophthalmopathy.
The numeric data were reported as the mean ± standard deviation.
[a]Statistical significance is indicated by *p* values less than 0.05.

Quantitative parameters between active and inactive phases

Active TAOs had significantly higher Dixon-EOM-SIR (4.26 ± 1.37 vs 2.61 ± 0.85, $p < 0.001$), fat-sat-EOM-SIR (3.50 ± 0.10 vs 2.30 ± 0.74, $p < 0.001$) and Dixon-WF-IF (0.10 ± 0.03 vs 0.08 ± 0.02, $p = 0.001$) as compared to inactive TAOs. Detailed comparisons between active and inactive TAOs were shown in Figure 3.

Staging performance for significant parameters

ROC curves analyses indicated that Dixon-EOM-SIR demonstrated the highest area under the curve (AUC) of 0.860 (cut-off, 3.32; sensitivity, 75.0%; specificity, 85.3%), followed by fat-sat-EOM-SIR (AUC, 0.852; cut-off, 2.99; sensitivity, 70.0%; specificity, 91.2%), and Dixon-IF-WF (AUC, 0.676; cut-off, 0.09; sensitivity, 70.0%; specificity, 67.6%). Dixon-EOM-SIR≥3.32 alone showed the highest diagnostic sensitivity for active TAOs (75.0%). After integrating Dixon-EOM-SIR ≥3.32 and Dixon-IF-WF ≥0.09, improved diagnostic efficiency and specificity were achieved (AUC, 0.872; specificity, 97.1%). ROC curves for the detailed staging efficiencies of significant parameters were shown in Figure 4.

Figure 2. Coronal Fat-sat T_2WI (a) and two-point Dixon T_2WI of water-only (b) in a 67-year-old female with active TAO. Coronal two-point Dixon T_2WI of water-only (b) showed better quality of FS than fat-sat T_2WI (a), especially in peri-inferior-EOM and temporal-facial regions. EOM, Extraocular muscle; fat-sat, fat saturation; T_2WI, T_2 weighted; TAO, thyroid-associated ophthalmopathy.

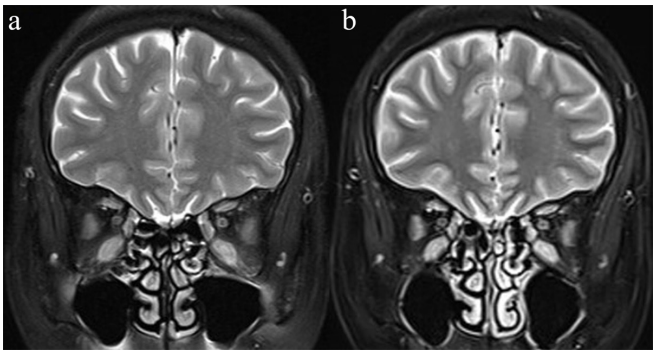

DISCUSSION

Our study illuminated two main findings. First, two-point Dixon T_2WI showed better quality of FS as well as higher EOM-SIR value than conventional fat-sat T_2WI. Second, two-point Dixon T_2WI exhibited both improved staging sensitivity and specificity for active TAOs compared with Fat-sat T_2WI. Our findings might provide relevant insight into the potency of Dixon technique in the utilization of TAO and other orbital diseases.

In this study, the two-point Dixon technique was superior to fat-sat technique in respect of overall image quality and FS uniformity in orbit, which was consistent with prior studies referring to lumbar and neck.[18,21] The conventional fat-sat technique is prone to poor quality of FS caused by magnetic field inhomogeneity. The magnetic inhomogeneity can shift the resonance frequencies of both water and lipid, resulting in errors during the frequency-selective process.[12] As a virtually water–fat separation method, Dixon technique was deemed to achieve improved homogeneity of FS and improved image quality with circumvention of magnetic field inhomogeneity.[15] In the present application regarding TAO, the improved FS efficiency, especially in peri-inferior EOM and temporal-facial regions by Dixon method, seemed to be even more significant, after considering the highest

Figure 3. Bar graph showing the comparisons of quantitative parameters between active and inactive TAOs. An asterisk indicates a significant difference (**$p < 0.001$, *$p < 0.01$). EOM, extraocular muscle; IF, intraorbital fat; SIR, signal intensity ratio; TAO, thyroid-associated ophthalmopathy; WF, water fraction.

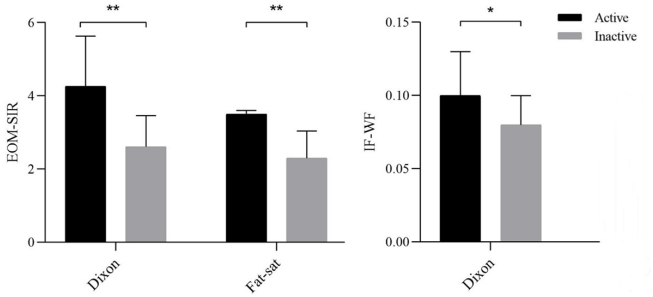

Figure 4. Receiver-operating characteristic curves of significant parameters for discriminating active TAOs. EOM, extraocular muscle; IF, intraorbital fat; SIR, signal intensity ratio; TAO, thyroid-associated ophthalmopathy; WF, water fraction.

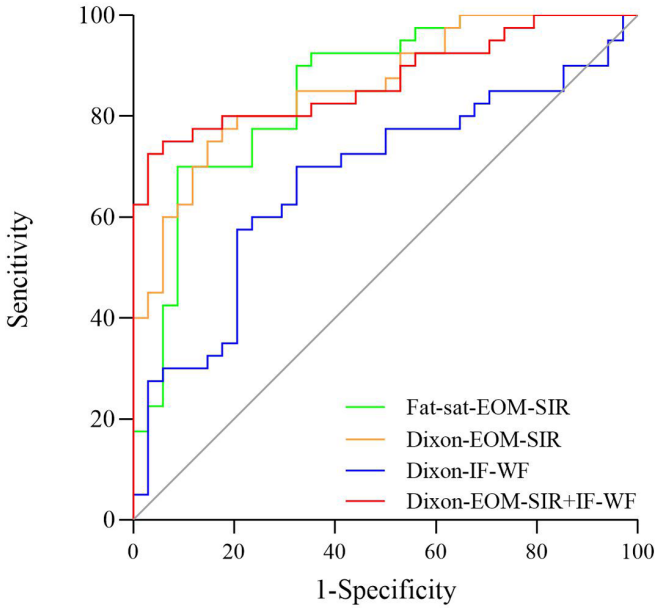

involvement rate of inferior EOM and the importance for the detection of internal high signal edema.[30,31]

Our study indicated that the EOM-SIRs generated from two-point Dixon T_2WI were significantly higher than those from fat-sat T_2WI. In the previous study of Gaddikeri et al[18], similar results were obtained during the comparison between Dixon and the other FS techniques of spectral presaturation with inversion recovery and STIR. Concerning the possible reason, the better quality of FS by Dixon method might be responsible. In our opinion, better FS would highlight the water signal to a greater extent. During our process of quantitative measurements, we found that the SIs of the edematous EOMs by Dixon technique were mostly higher than those by fat-sat technique, while the SIs of temporal muscles showed little difference between the two techniques. Therefore, it is reasonable that value of Dixon-EOM-SIR would be higher than that of fat-sat-EOM-SIR.

All the quantitative parameters of Dixon-EOM-SIR, fat-sat-EOM-SIR and Dixon-IF-WF increased significantly in active phase. The EOMs of the TAO patients in acute phase were histologically characterized by mononuclear cell infiltration, fibroblast proliferation, and edema in EOMs and intraorbital fat. By contrast, the EOMs were characterized by interstitial fibrosis and collagen deposition with minimal edema in inactive phase.[3,32,33] Different histological feature would lead to the corresponding change of quantitative metrics.

Further ROC curves analyses indicated that Dixon-EOM-SIR demonstrated higher AUC than fat-sat-EOM-SIR (0.860 *vs* 0.852), and also the highest diagnostic sensitivity for the active phase (75.0%). Integrating EOM-SIR and IF-WF derived from Dixon image, improved diagnostic efficiency and specificity could be achieved (AUC, 0.872; specificity, 97.1%). Base on the optimized image quality and elevated staging sensitivity and specificity demonstrated in our study, we suggest that the Dixon T_2WI could be used as a potent alternative beyond conventional sequence when assessing TAO patients in clinical practice.

Our study has several limitations. First, this is a retrospective study with relatively small study cohort. Further study with larger sample size is needed to verify our results. Second, only the two-point Dixon technique was applied because of the retrospective nature, which was relatively prone to phase error induced by field inhomogeneity. Further application of three- or multipoint Dixon techniques would help to correct this kind of error and generate more pure water-only and fat-only images.[15]

In conclusion, our study indicates that the two-point Dixon T_2WI offers better overall image quality, FS uniformity, as well as improved sensitivity and specificity in staging TAOs compared with conventional fat-sat technique. We suggest to use Dixon T_2WI technique to evaluate the patients with TAO in the daily practice.

FUNDING

This work was supported by National Natural Science Foundation of China (NSFC) (81801659 to Hao Hu).

DATA AVAILABILITY STATEMENT

The data that support the findings of this study are available from the corresponding author upon reasonable request.

REFERENCES

1. Şahlı E, Gündüz K. Thyroid-associated ophthalmopathy. *Turk J Ophthalmol* 2017; **47**: 94–105. doi: https://doi.org/10.4274/tjo.80688
2. Higashiyama T, Nishida Y, Ohji M. Changes of orbital tissue volumes and proptosis in patients with thyroid extraocular muscle swelling after methylprednisolone pulse therapy. *Jpn J Ophthalmol* 2015; **59**: 430–5. doi: https://doi.org/10.1007/s10384-015-0410-4
3. Gould DJ, Roth FS, Soparkar CNS. The diagnosis and treatment of thyroid-associated ophthalmopathy. *Aesthetic Plast Surg* 2012; **36**: 638–48. doi: https://doi.org/10.1007/s00266-011-9843-4
4. Kahaly G, Hansen C, Beyer J, Winand R. Plasma glycosaminoglycans in endocrine ophthalmopathy. *J Endocrinol Invest* 1994; **17**: 45–50. doi: https://doi.org/10.1007/BF03344962
5. Winand RJ, Cornet G, Etienne-Decerf J, Wadeleux P, Glinoer D. Original acquisition in the pathogenesis and the treatment of endocrine ophthalmopathy. *Metab Pediatr Syst Ophthalmol* 1988; **11**: 126–32.

6. Bartalena L, Pinchera A, Marcocci C. Management of Graves' ophthalmopathy: reality and perspectives. *Endocr Rev* 2000; **21**: 168–99. doi: https://doi.org/10.1210/er.21.2.168
7. Wippold FJ. Head and neck imaging: the role of CT and MRI. *J Magn Reson Imaging* 2007; **25**: 453–65. doi: https://doi.org/10.1002/jmri.20838
8. Mayer EJ, Fox DL, Herdman G, Hsuan J, Kabala J, Goddard P, et al. Signal intensity, clinical activity and cross-sectional areas on MRI scans in thyroid eye disease. *Eur J Radiol* 2005; **56**: 20–4. doi: https://doi.org/10.1016/j.ejrad.2005.03.027
9. Siakallis LC, Uddin JM, Miszkiel KA. Imaging investigation of thyroid eye disease. *Ophthalmic Plast Reconstr Surg* 2018; **34**(4S Suppl 1): S41–51. doi: https://doi.org/10.1097/IOP.0000000000001139
10. Cakirer S, Cakirer D, Basak M, Durmaz S, Altuntas Y, Yigit U. Evaluation of extraocular muscles in the edematous phase of Graves ophthalmopathy on contrast-enhanced fat-suppressed magnetic resonance imaging. *J Comput Assist Tomogr* 2004; **28**: 80–6. doi: https://doi.org/10.1097/00004728-200401000-00013
11. Hu H, Xu X-Q, Wu F-Y, Chen H-H, Su G-Y, Shen J, et al. Diagnosis and stage of Graves' ophthalmopathy: efficacy of quantitative measurements of the lacrimal gland based on 3-T magnetic resonance imaging. *Exp Ther Med* 2016; **12**: 725–9. doi: https://doi.org/10.3892/etm.2016.3389
12. Delfaut EM, Beltran J, Johnson G, Rousseau J, Marchandise X, Cotten A. Fat suppression in MR imaging: techniques and pitfalls. *Radiographics* 1999; **19**: 373–82. doi: https://doi.org/10.1148/radiographics.19.2.g99mr03373
13. Borges AR, Lufkin RB, Huang AY, Farahani K, Arnold AC. Frequency-selective fat suppression MR imaging. localized asymmetric failure of fat suppression mimicking orbital disease. *J Neuroophthalmol* 1997; **17**: 12–17.
14. Ma J, Jackson EF, Kumar AJ, Ginsberg LE. Improving fat-suppressed T2-weighted imaging of the head and neck with 2 fast spin-echo Dixon techniques: initial experiences. *AJNR Am J Neuroradiol* 2009; **30**: 42–5. doi: https://doi.org/10.3174/ajnr.A1132
15. Ma J. Dixon techniques for water and fat imaging. *J Magn Reson Imaging* 2008; **28**: 543–58. doi: https://doi.org/10.1002/jmri.21492
16. Ma J, Son JB, Zhou Y, Le-Petross H, Choi H. Fast spin-echo triple-echo Dixon (fTED) technique for efficient T2-weighted water and fat imaging. *Magn Reson Med* 2007; **58**: 103–9. doi: https://doi.org/10.1002/mrm.21268
17. Reeder SB, Wen Z, Yu H, Pineda AR, Gold GE, Markl M, et al. Multicoil Dixon chemical species separation with an iterative least-squares estimation method. *Magn Reson Med* 2004; **51**: 35–45. doi: https://doi.org/10.1002/mrm.10675
18. Gaddikeri S, Mossa-Basha M, Andre JB, Hippe DS, Anzai Y. Optimal fat suppression in head and neck MRI: comparison of multipoint Dixon with 2 different Fat-Suppression techniques, spectral presaturation and inversion recovery, and stir. *AJNR Am J Neuroradiol* 2018; **39**: 362–8. doi: https://doi.org/10.3174/ajnr.A5483
19. Kishida Y, Koyama H, Seki S, Yoshikawa T, Kyotani K, Okuaki T, et al. Comparison of fat suppression capability for chest MR imaging with Dixon, SPAIR and stir techniques at 3 tesla Mr system. *Magn Reson Imaging* 2018; **47**: 89–96. doi: https://doi.org/10.1016/j.mri.2017.11.012
20. Le Y, Kipfer HD, Majidi SS, Holz S, Lin C. Comparison of the artifacts caused by metallic implants in breast MRI using dual-echo Dixon versus conventional fat-suppression techniques. *AJR Am J Roentgenol* 2014; **203**: W307–14. doi: https://doi.org/10.2214/AJR.13.10791
21. Lee S, Choi DS, Shin HS, Baek HJ, Choi HC, Park SE. Fse T2-weighted two-point Dixon technique for fat suppression in the lumbar spine: comparison with SPAIR technique. *Diagn Interv Radiol* 2018; **24**: 175–80. doi: https://doi.org/10.5152/dir.2018.17320
22. Sinclair CDJ, Morrow JM, Yousry TA, Golay X, Thronton JS. Test-retest reproducibility of mtr, T2 and 3-point Dixon fat quantification methods in muscle MRI. *In Proc Intl Soc Magn Reson Med* 2011; **433**: 3958.
23. He Q, Weng D, Zhou X, Ni C. Regularized iterative reconstruction for undersampled blade and its applications in three-point Dixon water-fat separation. *Magn Reson Med* 2011; **65**: 1314–25. doi: https://doi.org/10.1002/mrm.22726
24. Tien RD. Fat-suppression MR imaging in neuroradiology: techniques and clinical application. *AJR Am J Roentgenol* 1992; **158**: 369–79. doi: https://doi.org/10.2214/ajr.158.2.1729800
25. Bartley GB, Gorman CA. Diagnostic criteria for Graves' ophthalmopathy. *Am J Ophthalmol* 1995; **119**: 792–5. doi: https://doi.org/10.1016/S0002-9394(14)72787-4
26. Mourits MP, Prummel MF, Wiersinga WM, Koornneef L. Clinical activity score as a guide in the management of patients with Graves' ophthalmopathy. *Clin Endocrinol* 1997; **47**: 9–14. doi: https://doi.org/10.1046/j.1365-2265.1997.2331047.x
27. Kirsch EC, Kaim AH, De Oliveira MG, von Arx G. Correlation of signal intensity ratio on orbital MRI-TIRM and clinical activity score as a possible predictor of therapy response in Graves' orbitopathy – a pilot study at 1.5 T. *Neuroradiology* 2010; **52**: 91–7. doi: https://doi.org/10.1007/s00234-009-0590-z
28. Kaichi Y, Tanitame K, Itakura H, Ohno H, Yoneda M, Takahashi Y, et al. Orbital fat volumetry and water fraction measurements using T2-weighted FSE-IDEAL imaging in patients with thyroid-associated orbitopathy. *AJNR Am J Neuroradiol* 2016; **37**: 2123–8. doi: https://doi.org/10.3174/ajnr.A4859
29. Armstrong RA. Statistical guidelines for the analysis of data obtained from one or both eyes. *Ophthalmic Physiol Opt* 2013; **33**: 7-14. doi: https://doi.org/10.1111/opo.12009
30. Higashiyama T, Nishida Y, Morino K, Ugi S, Nishio Y, Maegawa H, et al. Use of MRI signal intensity of extraocular muscles to evaluate methylprednisolone pulse therapy in thyroid-associated ophthalmopathy. *Jpn J Ophthalmol* 2015; **59**: 124–30. doi: https://doi.org/10.1007/s10384-014-0365-x
31. Chen W, Hu H, Chen H-H, Su G-Y, Yang T, Xu X-Q, et al. Utility of T2 mapping in the staging of thyroid-associated ophthalmopathy: efficiency of region of interest selection methods. *Acta Radiol***61**: 1512–9. doi: https://doi.org/10.1177/0284185120905032
32. Hiromatsu Y, Eguchi H, Tani J, Kasaoka M, Teshima Y. Graves' ophthalmopathy: epidemiology and natural history. *Intern Med* 2014; **53**: 353–60. doi: https://doi.org/10.2169/internalmedicine.53.1518
33. Ludgate M, Baker G. Unlocking the immunological mechanisms of orbital inflammation in thyroid eye disease. *Clin Exp Immunol* 2002; **127**: 193–8. doi: https://doi.org/10.1046/j.1365-2249.2002.01792.x